

# Wear-Resistant Bearings

Gary L. Doll and Michael N. Kotzalas

Reprinted courtesy The Timken Company

## Management Summary

Since the late 1990s, the Timken Company has employed surface engineering technologies on bearing rollers to provide wear resistance and friction reduction to demanding customer applications. More than a decade of intensive research and development has resulted in two new technologies that, when used in combination, expand the performance of rolling element bearings well beyond previous limits.

Timken's new surface engineering technologies were not developed to be temporary fixes, but were instead designed to address the root causes of the mechanisms responsible for life-limiting bearing wear. When rolling elements with these surface engineering technologies are incorporated into roller bearings, the bearing assembly is referred to as a Timken wear-resistant bearing.

**Surface engineering.** Surface engineering is the practice of altering the chemical and/or topographical proper-

ties of the surface of a component or device. Timken has previously shown that an engineered surface, which has worked well at reducing wear in rolling element bearings, is a metal-containing diamond-like carbon coating applied to super-finished rolling elements (Refs. 1–2). It is sometimes beneficial to consider real surfaces as having roughness on different length scales. So, whereas, quantities—such as Ra and Rq—describe longer length roughness characteristics, shorter length roughness is better quantified by a quantity such as asperity slope  $\Delta q$ .

A standard finish on a rolling element—typically one that has been ground and honed—produces a surface with a long-length scale roughness that in cross-section resembles the illustration labeled as “Standard” (Fig. 1). Ra and Rq values of 100 nm and 140 nm, respectively, are commonly measured on these surfaces. An illustration of a surface produced by a super-finishing process is also shown (Fig. 1).

These surfaces have typical Ra and Rq values of 60 nm and 90 nm, respectively. Surfaces with smaller Ra and Rq values promote greater separation of contacting surfaces and larger load-bearing capabilities that produce a more desirable distribution of contact stresses in the material than surfaces produced by standard finishing processes.

Analysis of the short-length scale roughness from measurements of ground, ground + honed, and super-finished surfaces yields average asperity slopes (Fig. 1). Because asperity interactions in contacting surfaces play an important role in wear modes—micro-pitting and smearing, for example—the smaller the asperity slope, the smaller the interaction.

A super-finishing process described by Hashimoto, et al. (Ref. 3) can produce surfaces such as that shown (Fig. 2), in which most of the traditional machining features have been removed. For comparison purposes, a standard surface that has been ground and honed is also shown. 3-D topographical profiles of each surface obtained by a white light interferometer microscope are shown below the optical images.

Super-finished surfaces are especially beneficial to mechanical components operating in boundary layer lubrication because the opportunities for asperity interactions in the contact areas are greatly reduced.

Metal-containing, diamond-like carbon (DLC) coatings were first developed by Dimigen (Ref. 4). Later, these materials were found to be nanocomposites consisting of metal carbide pre-

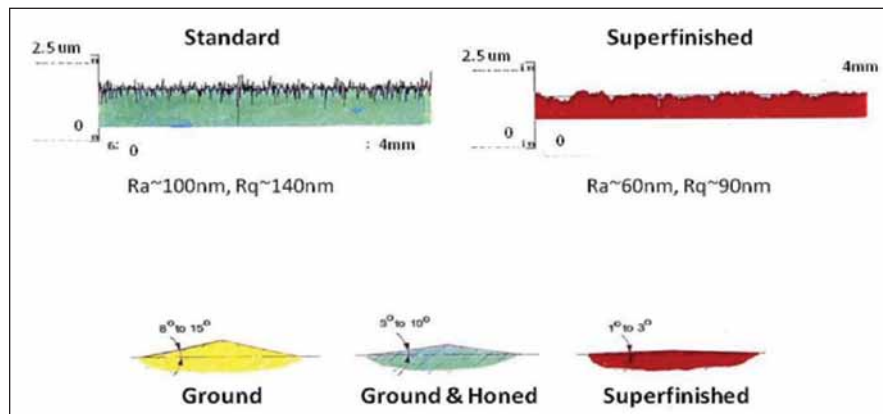


Figure 1—Roughness characteristics of finished rollers.

cipitates in amorphous hydrocarbon matrices (Ref. 5). Since tungsten containing diamond-like (W-DLC) coatings can usually be deposited at temperatures below the tempering points of engineering steels, they are currently utilized in many mechanical applications (Ref. 6). Generally, W-DLC coatings are two to three times harder than steel, use Cr adhesion layers, are less than three micrometers thick and have low friction coefficients when sliding against steel.

Like some other bearing manufacturers, Timken has used commercial coatings, such as W-DLC, for many years to provide wear resistance to rolling element bearings. For example, W-DLC coatings have been successfully used as barriers to the adhesive wear mechanisms that cause false brinelling and smearing in roller bearings. However, in boundary layer lubricated environments, W-DLC coatings have not exhibited the durability to remain intact for the entirety of a bearing's predicted life.

The lubrication environment that a bearing or other mechanical device operates in is commonly defined in terms of the dimensionless parameter  $\Lambda$  which is the ratio of the lubricant film thickness to the composite surface roughness of the contacting surfaces. Fatigue life testing was performed on tapered roller bearings with a commercial W-DLC coating applied to the rollers. A standard test protocol was used where bearings were operated at 150%-rated load, based upon 90 million revolutions, in a  $\Lambda=0.5$  lubrication regime, and in non-additized oil. Although the bearings with W-DLC coatings achieve their predicted lives at this lambda value, the W-DLC coatings on the rollers exhibited non-uniform wear. Images of the bodies and ends of these rollers are shown (Fig. 3). Whereas the coatings are still strongly adhered to the steel, fracture within the coating has generated non-uniform wear. Since the W-DLC is much harder than bearing steel, uneven wear of the roller coating is detrimental to the raceway surfaces.

After a detailed investigation probing the microstructures of W-DLC coatings, Timken was able to identify the defect in W-DLC responsible for

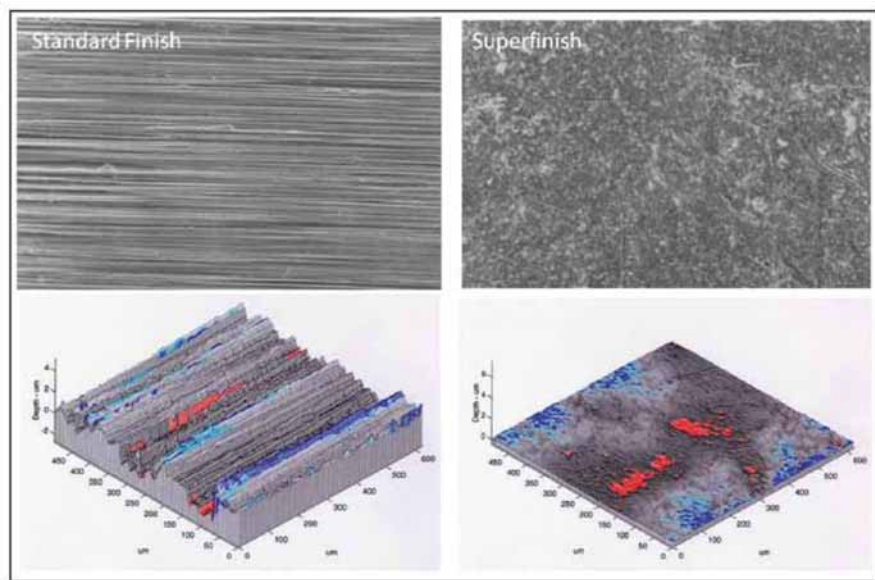


Figure 2—Optical images and their corresponding 3-D profiles of roller surfaces generated by standard (ground and honed) and super-finished processes.

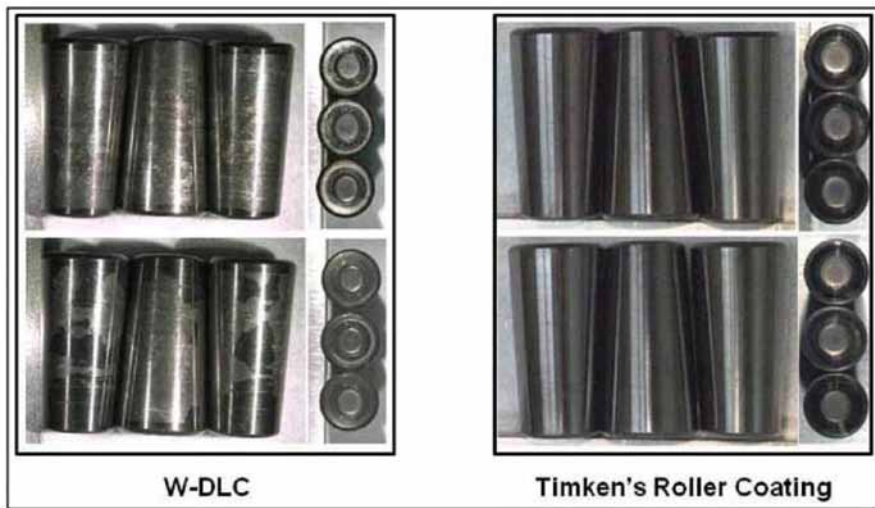


Figure 3—Comparison of the durability of commercial W-DLC and Timken's new roller coating.

the fracture-type wear and eliminate it through an optimization of the coating deposition process conditions. Bearings equipped with rollers with Timken's new coating were tested to their fatigue limits with the standard life test protocol described above. Rollers removed from the bearings at the end of the serviceable life of the bearing are also shown (Fig. 3). No visible coating wear is observed on either roller bodies or ends. Furthermore, coating thickness measurements performed prior and subsequent to the fatigue life tests are the same within the capabilities of the measurement system. This indicates that no measurable wear of the coating has occurred in this highly loaded, low lambda bearing environment.

**Wear resistance of bearings with engineered roller surfaces.** One of the life-limiting wear issues affecting main shaft and gearbox bearings in wind turbine generators is micropitting. Micropitting is caused by interaction of the raceway and roller residual finishing marks, or asperities, leading to high surface stresses in the contact. Normal stress alone is not typically sufficient to cause a crack to initiate at or very near the surface early in the lifecycle of a bearing. However, the addition of frictional shear stress increases the bulk contact stress values and brings the maximum values closer to the surface—as shown by Harris and Yu (Ref. 7)—allowing these localized stresses under the asperity contacts to become significant. This type of interac-

tion typically occurs when the lubricant film is insufficiently thick to separate the contacts and when there is relative sliding between the two contacting surfaces (Refs. 8–11).

Low-cycle micropitting is caused by high amounts of sliding between rollers and ring raceways, generating considerable shear stresses in the contact zone. From the viewpoint of an element-of-area on a ring raceway, the cyclic shear stresses imparted by each passing roller ultimately generate micro-cracks that propagate in the direction of the sliding shear stress on the slower moving com-

ponent (Refs. 12–13). As these micro-cracks propagate, pieces of the raceway begin to break away from the surface, leaving micrometer-size pits.

The evolution of low-cycle micropitting to raceway spalling of a 230/600 main-shaft spherical roller bearing is shown (Fig. 4). Figure 4-A shows the onset of micropitting, where two distinct wear tracks have emerged in the center of the raceway. As the micropitting continues, more and more material is worn away, leading to a loss of the design contact geometry in the center and increasingly higher stress concentrations at the

edges of the wear track. Fatigue spalls initiate at these areas of high geometric stress concentrations and propagate on raceways like that shown in Figure 4-B.

The raceway spalling of these bearings is not due to classic surface-initiated or inclusion-related fatigue on which the predicted bearing life is calculated, but is due instead to the loss of the designed contact geometry due to micropitting wear and a concomitant increase in geometric stress concentrations at the edges of the roller/raceway contact. Since there exists a high amount of sliding between the rollers and raceways in a spherical roller bearing, it is not unusual to observe micropitting wear of these bearings in low-lambda conditions. For example, images of spherical roller bearing raceways that have been fatigue life tested at low lambda ( $\Lambda \sim 0.5$ ) are shown (Fig. 5).

To stimulate early fatigue, both bearings were deliberately damaged with steel debris prior to life testing. The top image shows a raceway that ran against uncoated steel rollers, with the gray band of micropitting clearly visible. No indication of micropitting is observed on the raceway in the bottom image that ran against rollers with Timken's engineered surfaces. Clearly, a significant reduction in the shear stresses between rolling elements and ring raceways can eliminate the mechanisms responsible for low-cycle micropitting in roller bearings.

Another wear mode that damages bearings in applications like wind turbine gearbox is smearing. Like micropitting, smearing in bearings also occurs when rollers are skidding against raceways in low-lambda conditions. But, whereas micropitting is a microscopic surface fatigue mechanism, smearing occurs when the heat from the friction between the sliding rollers and the raceways generates local temperatures in the contact zone high enough to melt the steel surfaces. The large-scale plasticization and localized melting generates a smeared appearance on the raceway surface. FeO is sometimes found in the smeared wear patch, which indicates that the local temperature in the contact zone exceeded  $\sim 550^{\circ}\text{C}$ .

A simple bench test has been performed to demonstrate the ability of

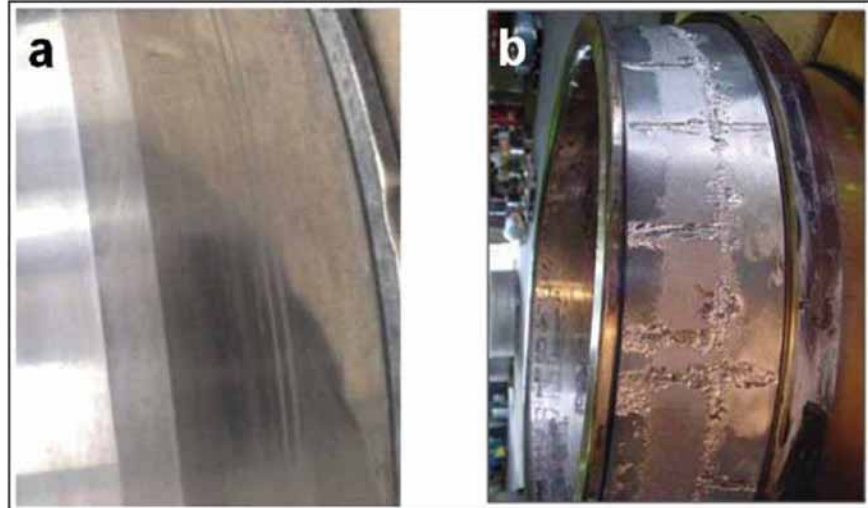


Figure 4—(A) Onset of micropitting leading to failure of a (B) wind turbine main-shaft spherical roller bearing.



Figure 5—Debris-damaged spherical roller bearings after fatigue life testing in low-lambda. Although micropitting is clearly evident on the ring raceways that ran against uncoated steel rollers, no micropitting occurred on the raceways running against rollers with Timken's engineered surfaces.

Timken's engineered surface (ES) to inhibit smearing or scuffing-type wear. In this test, two highly loaded steel rings were placed into contact with 150% slide/roll ratio and the lubricant entrainment velocity was reduced in stages until a spike in the frictional torque was observed. In one experiment untreated steel rings were used; in the other, a steel ring with an engineered surface was run against an as-ground ring. Images of the ring pairs are displayed (Fig. 6).

The pair of as-ground steel rings experienced smearing wear that progressed very rapidly to galling. However, since no frictional torque spike was observed while the ES-treated ring ran against the as-ground steel ring, it is concluded that smearing wear did not occur within the load and speed limits of this experiment. Examination of the ES-treated ring surface indicates no visual signs of wear. Since no smearing occurred when the ES-treated ring ran against the as-ground steel ring, the frictional heating at that interface must have been considerably lower than in the contact zone of the untreated steel rings.

Debris damage is another wear mode known to affect bearing life. As indicated (Fig. 5), the debris damage of the spherical roller bearings made from through-hardened AISI 52100 reduced the actual life of the bearings with untreated rollers by between 30–40%. However, the same debris damage on an identical spherical roller bearing with ES-treated rollers suffered no statistical reduction in life.

Another laboratory-scale test was constructed to quantify effects of debris damage on the actual lives of case-carburized tapered roller bearings. In this test, bearings were rotated under load for a specific duration in AISI 52100 debris-laden oil. The debris particle sizes were between 25 and 53  $\mu\text{m}$  with a 0.5 mg/ml concentration in the SAE 10-weight lubricant. Next, the bearings were solvent cleaned to remove the debris. Finally, the bearings were life-tested using a first-in-four failure criterion in clean SAE 10-weight oil.

Statistically significant populations of bearings with untreated rollers and bearings with ES-treated rollers were tested. Results of those tests are shown (Fig. 7) where the  $L_{16}$  values and upper

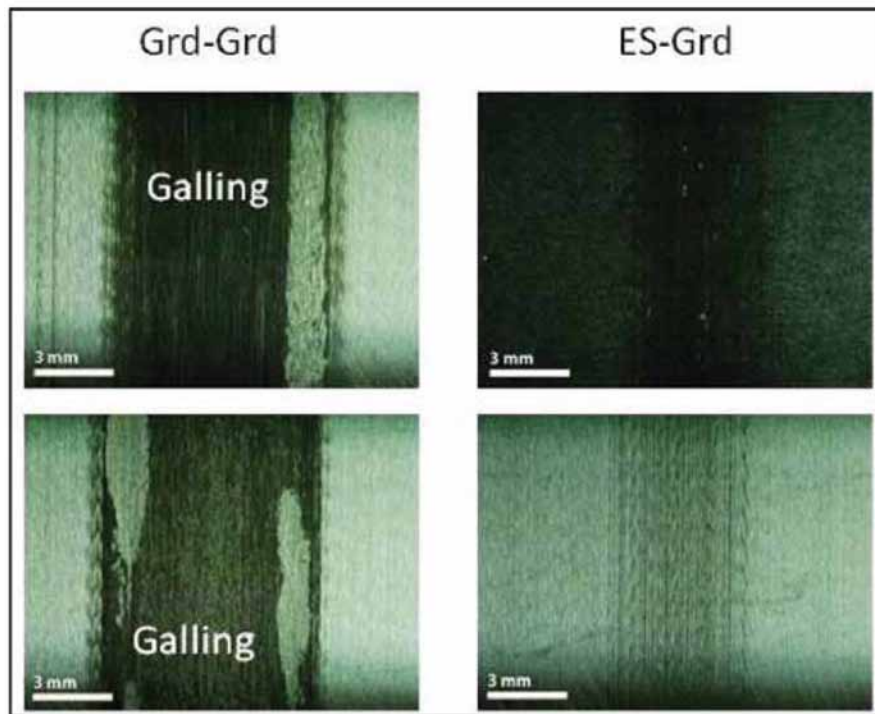


Figure 6—Smearing wear testing of ground steel surfaces against steel and ES-treated surfaces.

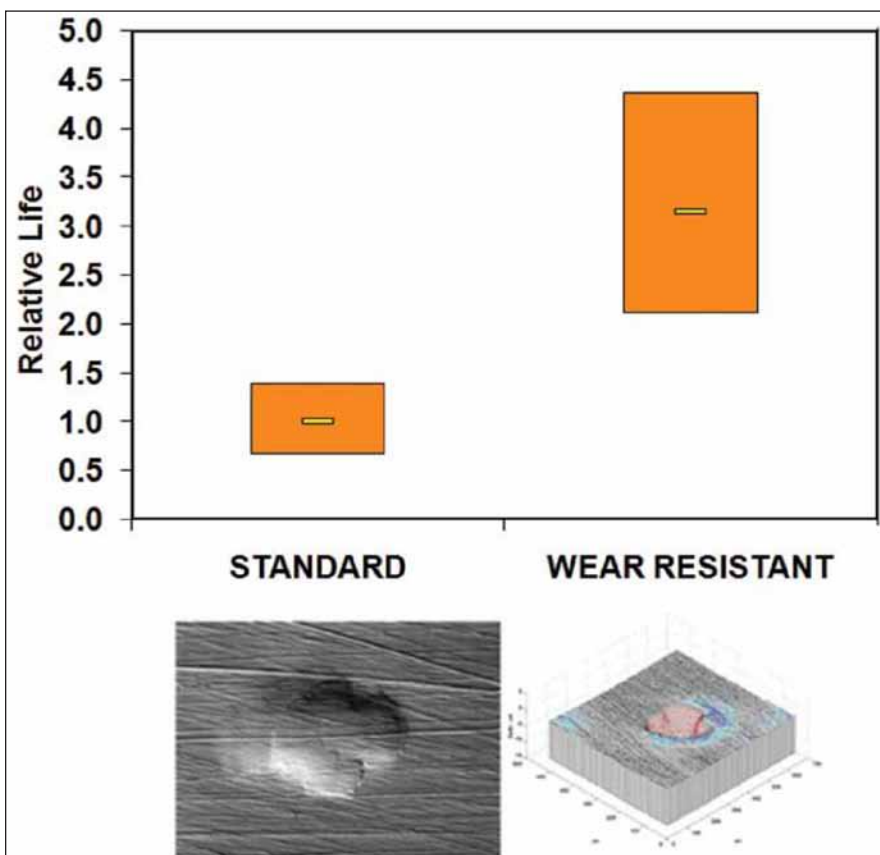


Figure 7—Life test results of debris-damaged, case-carburized standard and wear-resistant tapered roller bearings. Also shown: (left) optical image of a debris dent in a raceway and (right) a 3-D surface profile of that dent showing raised crater rims resulting from plastic flow of the steel during the creation of the dent.

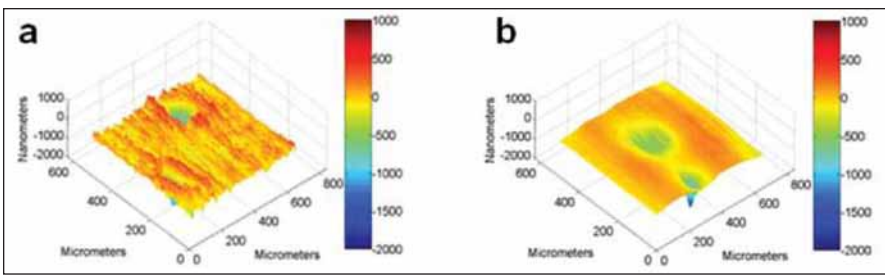


Figure 8—3-D profile topographies of debris dents on bearing raceways measured after life testing. The image of the debris dent in "A" is from a raceway that ran against untreated steel rollers, and shows that the raised edges around the crater formed from the debris are still in place. On the other hand, the image of the debris dent in "B" is from a raceway that ran against ES-treated rollers. All traces of the raised edges have been removed, as have the residual grinding lines. It is the ability of the ES-treated rollers' ability to remove the raised edges around debris craters that negates the fatigue life-reducing mechanism associated with debris-damaged raceways.

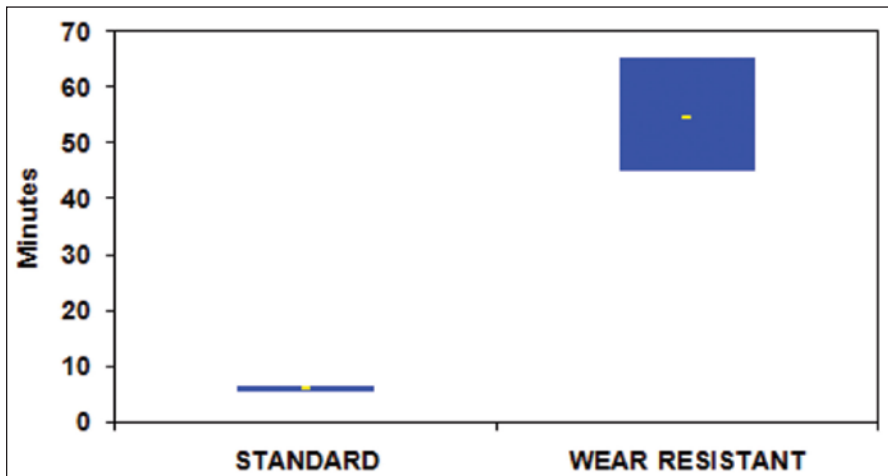


Figure 9—Results of a lubricant starvation test on tapered roller bearings with standard rollers and ES-treated roller ends. The ES treatments on the roller-ends provided a barrier to the adhesive wear that causes scuffing and scoring, and allowed the bearings to operate under full loads and speeds approximately nine times longer than identical bearings with standard rollers.

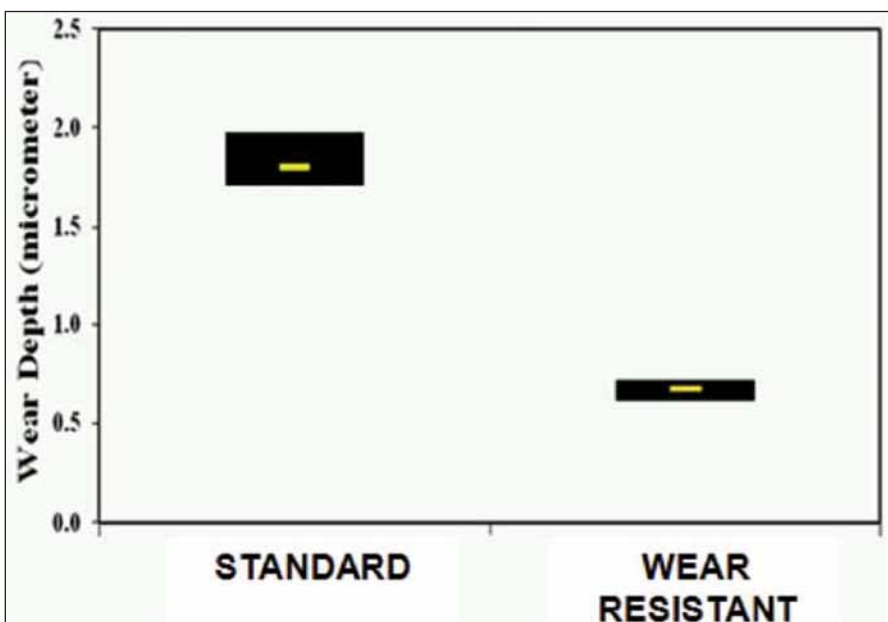


Figure 10—Result of a bench test designed to evaluate the ability of ES-treated rollers to address the adhesive wear that causes false brinelling. Unlike standard bearings, wear-resistant bearings with ES-treated rollers did not exhibit wear from false brinelling.

and lower 65% confidence bands (tops and bottoms of the bars) are normalized to the baseline test results. Since the fracture toughness of case-carburized steel is two to three times that of through-hardened steel (Ref. 14), the reduction in the lives of (equivalent) case-carburized bearings due to debris damage is less than that of through-hardened bearings. Also shown in the figure is an optical image of a debris dent in a bearing raceway and a 3-D surface profile of the dent. Statistically, the bearings with the ES-treated rollers had an  $L_{16}$  life more than three times greater than the life of identical bearings with untreated rollers.

The mechanism by which ES-treated rollers make bearings tolerant to debris damage is clearly illustrated (Fig. 8). The image of the debris dent (Fig. 8-A) is from a raceway that ran against untreated steel rollers and shows that the raised edges around the crater formed from the debris are still in place. On the other hand, the image of the debris dent (Fig. 8-B) is from a raceway that ran against ES-treated rollers. All traces of the raised edges have been removed as have the residual grinding lines. It is the ability of the ES-treated rollers to remove the raised edges around debris craters that negates the fatigue-life-reducing mechanism associated with debris-damaged raceways.

Due to large entrainment velocities, thick lubricant films usually exist at the rib-roller end-sliding contact of a tapered roller bearing. Situations occasionally occur where the lubricant film at this interface is insufficient to separate the asperities of the roller end and rib face. In these situations, adhesive wear between the asperities can lead to scuffing, scoring and, eventually, galling. Examples of situations where this adhesive wear can occur include the use of ultra-low-viscosity lubricants, large axial loads, highly loaded high-speed operation and lubricant interruption or loss.

A laboratory test was devised to measure the resistance to rib-roller end-failure of tapered roller bearings with ES-treated roller ends. The test was designed to mimic a field condition where bearings in gearboxes experienced an extended lubrication loss condition. Test bearings were immersed in

a solution containing 80% hexane and 20% GL-5 gear oil. Upon removal from the solution, the hexane was allowed to evaporate, leaving behind a thin oil film on the bearing surfaces.

Figure 9 displays the time to rib-roller end scuffing for bearings with and without ES-treated roller ends. At least 25 bearings were tested for each condition; results were analyzed using first-in-one Weibull statistics and 90% confidence bands were calculated around L50 lives. Whereas uncoated baseline bearings had an L50 value of about six minutes, bearings with ES-treated roller ends had L50 values of about 50 minutes.

The ES treatments on the roller ends provided a barrier to the adhesive wear that causes scuffing and scoring, thus allowing the bearings to operate under full loads and speeds of up to nine times longer than identical bearings with standard rollers. Wear-resistant bearings with ES-treated rollers are currently being used in the metal forming and agricultural industries, as well as in flight-critical aerospace systems.

False brinelling or fretting is an adhesive wear mechanism that can occur between rolling elements and races whenever a non-rotating bearing is subjected to external vibration. Under these conditions lubricant is squeezed from between the contacts and the relative motion of the surfaces is too small for the lubricant to be replenished. Natural oxide films that normally protect steel surfaces are removed, permitting metal-to-metal contact and causing adhesion of surface asperities.

Fretting begins with an incubation period during which the wear mechanism is mild adhesion and the wear debris is magnetite ( $Fe_3O_4$ ). Damage during this incubation period is referred to as false brinelling. If wear debris accumulates in amounts sufficient to inhibit lubricant from reaching the contact, then the wear mechanism becomes severe adhesion that breaks through the natural oxide layer and forms strong welds with the steel. In this situation the wear rate increases dramatically and damage escalates to fretting corrosion. Relative motion breaks welded asperities and generates hematite ( $\alpha$ -

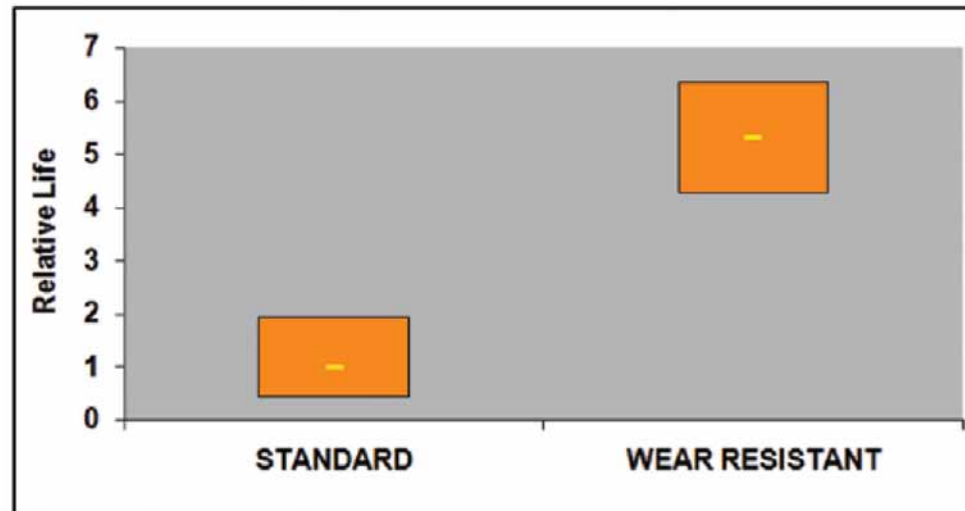


Figure 11—Results of life testing of standard bearings and wear-resistant bearings with ES-treated rollers in a low-lambda lubrication environment. The relative life of wear-resistant bearings is more than three times greater than standard bearings at  $\Delta=0.5$  lubrication conditions.

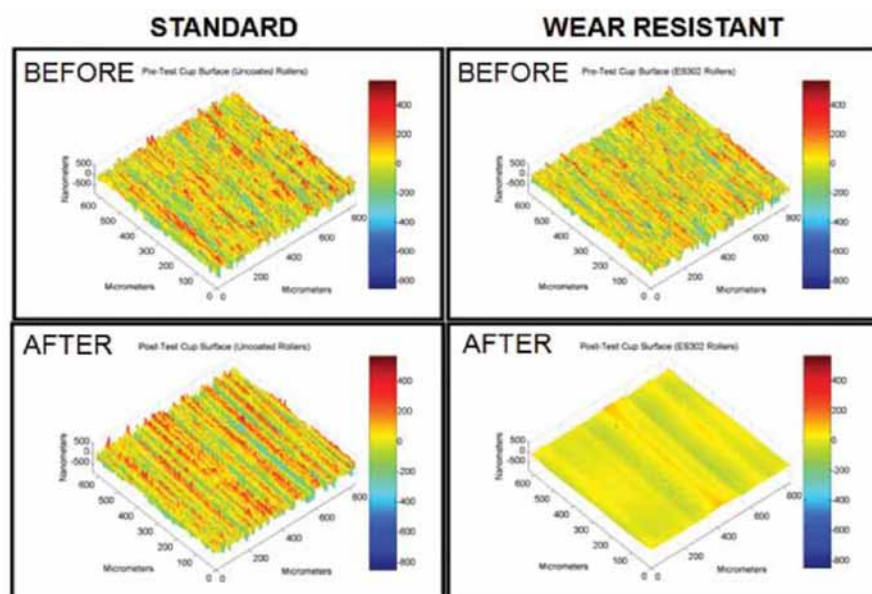


Figure 12—3-D topographical profiles of standard and wear-resistant bearing raceway surfaces before and after completing 44 million revolutions at 150%-rated loads.

$Fe_2O_3$ )—a fine powder, reddish-brown in color.

A laboratory-scale testing apparatus was designed to evaluate the ability of ES-treated rollers to inhibit false brinelling in bearings. Standard bearings with steel rollers and wear-resistant bearings with ES-treated rollers were tested. All bearings were lubricated with GL-4 transmission gear oil before testing. The test apparatus applied an oscillating 18.7 kN axial load to the bearings for 500,000 oscillations—conditions identical to a bearing application that experienced false brinelling in the field.

Subsequent to testing, depths of the grooves produced on the outer race were

measured. Figure 10 displays the average wear depths and standard deviations for the standard and wear-resistant bearings. After testing, the standard bearings exhibited grooves on the raceways with average depths of 1.85  $\mu m$ . On the other hand, the wear-resistant bearings had average groove depths of only 0.68  $\mu m$ . The wear of the raceway oscillating against the ES-treated rollers was very slight and appeared to be caused by gentle lapping rather than adhesive wear.

Examples of applications that use wear-resistant bearings to eliminate false brinelling include off-road truck

transmissions, rolling mills, tractors and wind turbines.

**Low  $\Lambda$  fatigue life of bearings with engineered roller surfaces.** Bearings have generally been selected according to the dynamic and static load ratings. The dynamic load rating  $C_1$  is a measure of the bearing's ability to withstand rolling contact fatigue, which by typical industry practice is according to the ISO load and life rating standard (Ref. 15). The static load rating  $C_0$  is a measure of the bearing's ability to withstand the maximum-applied load without function-reducing, permanent deformations or bearing ring destruction according to ISO standard 76 (Ref. 16). The dynamic load rating is used in the ISO 281 standard life rating equation for roller bearings:

$$L_{nm} = a_1 a_{ISO} \left( \frac{C_1}{P} \right)^{10.3} \quad (1)$$

where:

$a_1$  is the life modification factor for reliability,

$a_{ISO}$  is the integrated life modification factor accounting for material, lubrication and hard particle contamination,

and  $L_{nm}$  is the modified rating life in millions of revolutions.

Nominally, roller bearing endurance is calculated as  $L_{10}$ , the rolling contact fatigue life in millions of revolutions that 90% of the bearings will survive. Detailed calculations to predict  $a_{ISO}$  are given by Harris, et al. (Ref. 17) and indicate that if a roller bearing is operated in low-lambda conditions ( $\Lambda < 1$ ),  $a_{ISO}$  and  $L_{10}$  become small.

Full-scale life testing has been performed on standard and wear-resistant bearings with ES-treated rollers in  $\Lambda$  0.5 conditions. All bearings were life-tested using a first-in-four failure criterion in clean SAE 10-weight oil at 150%-rated load at 90 million cycles.

Statistically significant populations of standard and wear-resistant bearings were tested. Results of the  $\Lambda = 0.5$  tests are shown (Fig. 11) where the  $L_{10}$  values and upper and lower 65% confidence bands (tops and bottoms of the bars) are normalized to the standard bearing test results.

As indicated (Fig. 11), the relative  $L_{10}$  life of the wear-resistant bearing with ES-treated rollers is more than five times that of a standard bearing operating in low-lambda conditions.

The mechanism by which this large boost in low lambda bearing life is achieved is revealed in an examination of the 3-D topographic profiles of the raceway surfaces in Figure 12. In the low-lambda life test described above, one standard and one wear-resistant bearing were removed from testing after about 44 million cycles, and the raceways of the outer rings were measured by 3-D optical profilometry. Whereas the topography of the raceway of the standard bearing remained essentially unchanged after 44 million cycles, the raceway of the wear-resistant bearing has been highly polished.

Calculations based upon this highly polished surface and the Hamrock-Dowson (Ref. 18) lubricant film thickness yield a lambda value greater than two. Therefore, although the lambda value calculated from the initial surface parameters was 0.5, the ES-treated rollers have dramatically polished the raceways such that the wear-resistant bearing is effectively operating in an elastohydrodynamic  $\Lambda \sim 2$  regime.

## Summary

Table 1 summarizes the application advantages of wear-resistant bearings with ES-treated rollers. Since bearings seldom operate in fully lubricated environments, they rarely experience the number of cycles for which they were

designed. In low-lambda situations the ES-treated rollers in wear-resistant bearings polish the ring raceways—effectively increasing the separation of the contacting asperities. This polishing action continues until the contacts are fully separated by the lubricant film and the bearing is no longer operating in a low-lambda situation.

Interruption of the supply of lubricant to bearings can result in adhesive wear between the rollers and contacting surfaces on rings. Depending upon the loads and speeds, the adhesive wear rates increase until scuffing, scoring or galling occurs. ES treatments on rollers will not participate in adhesive wear with raceway asperities, but if the loads and speeds in the contacting areas are large enough and the lubricant interruption is long enough, the coating on the rollers will wear through graphitization. However, once the coating is worn away, adhesive wear ensues; while the coating is wearing, it allows the bearing to remain operational.

Abrasive particles that pass through worn seals that were not removed after manufacture—or are generated by wear of other components—can damage bearing surfaces if the particles are larger than the lubricant film. Depending on the hardness and brittleness of the particle, they can generate dents on the raceway and/or roller surface. During the denting process, displaced material creates shoulders around the debris crater. When these raised shoulders come into the contact zone of a bearing, very high, sub-surface stresses are generated and fatigue cracks initiate at low stress cycles (Ref. 19).

Because the ES treatments on the rollers of wear-resistant bearings are twice as hard as the steel raceways, they remove these shoulders through the same kind of polishing action described above. As a result, the stress risers that

**Table 1—Summary of advantages ES-treated rollers provide to wear-resistant bearings**

ADVANTAGE	WEAR-RESISTANT BEARINGS
Enhanced low $\Lambda$ fatigue life	Specially designed rollers polish the raceways, reducing Ra and increasing $\Lambda$ .
Scoring resistance from loss of lubrication	Rollers in wear-resistant bearings form barriers to adhesive wear during periods of lubricant starvation.
Debris tolerance	Rollers in wear-resistant bearings remove shoulders around debris generated craters on raceways and reduce surface roughness of ring raceways.
Resistant to smearing, micropitting, and fretting	Wear-resistant bearing rollers defeat the adhesive wear mechanisms that cause smearing, micropitting, and fretting.
Increased efficiency	Wear-resistant bearing rollers polish ring raceways, reducing surface roughness, increasing $\Lambda$ , reducing rolling torque, and increasing efficiency.

can cause early fatigue crack initiation are removed, thereby allowing the bearing to operate much longer than it otherwise would.

When lubricant film is insufficient to keep loaded steel surfaces in relative motion from coming into contact, adhesive wear occurs. If high loads are applied to skidding rollers, the frictional heating from the adhesive interaction of contacting asperities can increase the temperature in the contact zone to the point where the steel actually melts. This melting and subsequent re-solidification process weakens the steel and creates a smeared appearance when it occurs on bearing raceways.

The shear stresses from moderate loads applied to skidding rollers can create bearing damage known as micropitting. Very high transient loads applied to skidding rollers can generate near-surface stresses on non-metallic inclusions, creating cracks that propagate and remove thin pieces of the raceway. This type of damage is known as brittle flaking. ES treatments on wear-resistant bearings provide a barrier against the ability of raceway asperities to bond to the roller and reduce the shear stresses and frictional heating from skidding rollers that cause these bearing damage modes. By decreasing the shear stresses of skidding rollers, the maximum contact stress is driven deeper into the raceway, well beyond the region where cracks that cause brittle flaking originate.

Roller bearings with smooth raceways exhibit less frictional torque than bearings with rougher raceways. Since the ES-treated rollers in wear-resistant bearings continuously polish the raceways, the contribution of frictional torque from contacting asperities is eliminated in operation. Depending upon the application and the type of bearing, raceway polishing by ES-treated rollers can reduce parasitic bearing losses between 5–10%. 

## References

- Doll, G.L. and B.K. Osborn. "Engineering Surfaces of Precision Steel Components," *Proceedings Annual Technical Conference—Society of Vacuum Coaters*, 44, pp. 78–84, 2001.
- Doll, G.L., C.R. Ribaudo and R.D. Evans. "Engineered Surfaces for Steel Rolling Element Bearings and Gears," *Materials Science and Technology*, 2, pp. 367–374, 2004.
- Hashimoto, F., S.N. Melkote, R. Singh and R. Kalil. "Effect of Finishing Methods on Surface Characteristics and Performance of Precision Components in Rolling/ Sliding Contact," *International Journal of Machining and Machinability of Materials*, v. 6, pp. 3–15, 2009.
- Dimigen, H. and H. Hubsch. Carbon-Containing Sliding Layer, US Patent No. 4,525,417, 1985.
- Sjostrom, H., L. Hultman, J.-E Sundgren and L.R. Wallenberg. "Microstructure of Amorphous C-H and Metal-Containing C-H Films Deposited Onto Steel Substrates," *Thin Solid Films*, v. 23, pp. 169–179, 1993.
- Holmberg, K. and A. Matthews. *Coatings Tribology: Properties, Mechanisms, Techniques and Applications in Surface Engineering, Second Edition*, (Elsevier, Amsterdam), pp. 383–435, 2009.
- Harris, T. and W. Yu. "Lundberg–Palmgren Fatigue Theory: Considerations of Failure Stress and Stressed Volume," *Transactions ASME Journal of Tribology*, v. 121, n. 1, pp. 85–89, 1999.
- Averbach, B. and E. Bamberger. "Analysis of Bearing Incidents in Aircraft Gas Turbine Mainshaft Bearings," *Tribology Transactions*, v. 34, n. 2, pp. 241–247, 1991.
- Ueda, T., K. Ueda and N. Mitamura, "Unique Fatigue Failure of Spherical Roller Bearings and Life-Enhancing Measures," *Proceedings of the World Tribology Congress*, Washington D.C., Sept 12–16, 2005.
- Webster, M. and C. Norbart. "An Experimental Investigation of Micropitting Using a Roll Disk Machine," *Tribology Transactions*, v. 38, n. 4, pp. 883–893, 1995.
- Chiu, Y. (1997), "The Mechanism of Bearing Surface Fatigue: Experiments and Theories," *Tribology Transactions*, v. 40, n. 4, pp. 658–666, 1997.
- Ueda, T., K. Ueda and N. Mitamura. "Unique Fatigue Failure of Spherical Roller Bearings and Life-Enhancing Measures," *Proceedings of the World Tribology Congress*, Washington D.C., Sept 12–16, 2005.
- Webster, M. and C. Norbart. "An Experimental Investigation of Micropitting Using a Roll Disk Machine," *Tribology Transactions*, v. 38, n. 4, p. 883–893, 1995.
- Burrier, H. "Bearing Steels," *ASM Handbook Vol. 1: Properties and Selection: Irons, Steels and High-Performance Alloys*, ASM, Materials Park, Ohio, 380–388, 1990.
- Rolling Bearings: Dynamic Load Ratings and Rating Life, International Organization for Standards: International Standard ISO 281, 2007.
- Rolling Bearings: Static Load Ratings, International Organization for Standards, International Standard ISO 76, 2006.
- Harris, T. A., J.H. Rumbarger and C.P. Butterfield. "Wind Turbine Design Guide DG03: Yaw and Pitch Rolling Bearing Life," Technical Report NREL/TP-500-42362, U.S. National Renewable Energy Laboratory, Golden, CO, 2009.
- Hamrock, B. J. and D. Dawson. *Ball Bearing Lubrication*, Wiley, London, 1981.
- Biboulet, N. "Influence of Indentations on Rolling Bearing Life," Doctoral Thesis in Mechanical Engineering, INSA Lyon, 2008.